THE USE OF EXPERIMENTAL APPROACHES OF RADIATION PHYSICS TO THE INVESTIGATION ON EXPLOSIVE PROCESSES[1]

Boris P. Aduev, Eduard D. Aluker, Alexandr G. Krechetov and Yury A. Zakharov
Kemerovo State University, Kemerovo, Russia

A real-time investigation of the explosive decomposition of heavy-metal azides is reported. A multichannel instrument configuration designed specifically for the goals of the study is described; it is capable of measuring the transient conductivity and the spectral and kinetic characteristics of the luminescence and absorption of exploding samples with nanosecond and subnanosecond time resolution. New phenomena are discovered and analyzed: the predetonation conductivity and predetonation luminescence of heavy-metal azides. The conductivity of silver azide in the predetonation state is used to make an experimentally justified decision as to whether the explosion is driven by a thermal or chain mechanism, in favor of the latter. The sum-total of the new data provides the basis for the development of an experimentally justified model of predetonation luminescence.

1. INTRODUCTION

For close to half a century now scientists have been intrigued by the explosive decomposition of heavy-metal azides (HMAs)[1]. The applied aspect of this unflagging interest is related to the fact that the HMAs are the simplest and, hence, the most exhaustively studied representatives of initiating agents and serve as a model object for this class of systems[2].

The theoretical aspect of the problem runs much deeper. Until recently it has been impossible to reliably detect a single instance of a branched chain reaction involving quasi-particles in a solid. The explosive decomposition of HMAs is indeed of major interest from this perspective[3, 4].

By the early eighties a wealth of experimental data had been accumulated, and basic notions as to the mechanism underlying the explosive decomposition of HMAs had been formulated (see the survey in Ref. 2), laying the foundation for the majority of subsequent research on the problem.[5,6] In our opinion, however, an analysis of these experimental data and the explosive decomposition models developed from them justify a lingering sense of dissatisfaction.

Culling out papers aimed at narrowly confined applications, we discern two experimental approaches to the study of the explosive decomposition of HMAs.

1. The first approach is to investigate slow HMA decomposition processes in exposure to heat, light, ionizing radiations. electric fields, and magnetic fields.[6] Obviously, the applicability of data from these studies for the construction of a realistic model of explosive decomposition is highly problematical.[3,4]

2. The second approach involves experiments designed to investigate explosive decomposition directly. These experiments are set up according to the following scheme.[2,7] An explosion is initiated by an impulsive action (shock, a light pulse, an accelerator pulse, etc.). The goal is then to record either the event of an explosion[2] or, better, the time interval (induction period) between the initiating pulse and the instant of explosion as determined from me accompanying flash of light[7] or fragmentation of

[1] The present work has received financial support from the Russian Fund for Fundamental Research (# 01-03-32015a) and ISTC (# 2180).

the sample (using high-speed motion pictures).[2] Clearly, in this experimental setup only certain global parameters of the process are recorded, and the main event is excluded from the researcher's field of vision, viz.: the changes in the characteristics of the sample (or phenomena accompanying these changes) during the evolution of explosive decomposition.

We suppose that the only way to progress in understanding the mechanism of explosive decomposition of HMAs is the development of new experimental approaches that can be used to record in real time the variations of the characteristics (physical properties) of a sample during an explosion. As the foundation for such an experimental approach we have adopted pulse techniques used in radiation physics, [8] modifying them as necessary in application to the specific attributes of the investigation of explosive samples. The results of the implementation of this approach make up the content of the present article.

2. TECHNIQUE

The objects chosen for the investigation were azides of silver AgN_3, thallium TlN_3, and lead $Pb(N_3)_2$. The azides were prepared in powder form by dual-Jet crystallization.[9] The concentrations of the main impurities (Fe, Si, Ca, Mg, Al, Na) were determined polarographically and by complexometric analysis; they were less than 10^{16} - 10^{17} cm^{-3}.

The investigated thallium and lead azide samples were pressed tablets of diameter 10 mm and thickness 300-400 μm for the thallium azide and 2.5 mm and 30-40 μm for the lead azide. The silver azide samples were whiskers with characteristic dimensions 0,1×0,05× 10 mm^3 and "macrocrystals" with characteristic dimensions 0,5×3×3 mm^3. The crystals were grown from solution by a procedure described in Ref. 9. The density of cation vacancies in the crystals was less than 10^{16} cm^{-3} (Ref. 9).

The instrument configuration used in the study (Fig. 1) is based on the principles of experimental pulsed radiolysis and photolysis techniques.[8]

The sources of excitation (initiation) are a GIN-600 high-current electron accelerator (effective electron energy 300 keV, current density 1000 A/cm^2, and pulse duration 3 ns) and a YAG:Nd^{3+} laser (λ= 1064 nm, pulse duration 30 ps, and pulse energy 0.5-30 mJ).

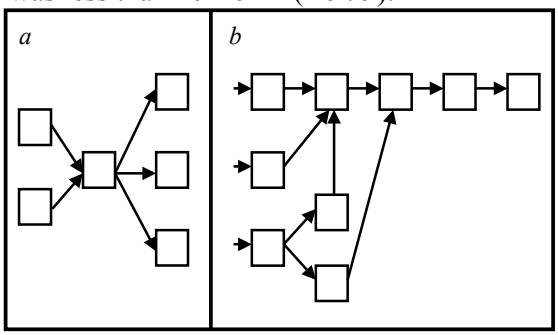

Fig. 1. The scheme of apparatus for the investigating the explosive decomposition.
a – the general scheme of apparatus:
1 –sample, 2 – excitation source (laser, electron accelerator) 3 –source of probing light, 4, 5, 6 – registration channels of optical, acoustic and electrical signals, respectively.
b – the scheme of signal registration channels:
1 – acoustic detector, 2 – oscillograph, 3 – television reading device, 4 – interface, 5 – computer, 6 – conductivity measuring cell, 7 – spectral device (monochromator, spectrograph) 8 – photomultiplier, 9 – streak camera.

The recording apparatus is made up of several synchronized channels. The optical channel consists of an ISP-51 spectrograph or MSD-1 monochromator and a photomultiplier (FEU-97, FEU-165-1, 14 ELU-FM) or FER-7 image-converter streak camera. The photomultiplier output signal is sent to the input of an oscilloscope (S7-8, S7-19): the output of the streak camera is sent through a television counting device utilizing an LI-702 Superkremnikon (a highly sensitive image iconoscope) and then

through an interface directly into a computer for processing. The spectral range spanned by the optical channel is 250-1000 nm, and the time resolution is 10 ns or better. Using streak-camera "View 2A" allows us to attain the time resolution ≤ 100 ps. By using a spectrograph-chronograph system (instead of the usual monochromator-photomultiplier combination) in the optical channel it is possible to obtain the relaxation pattern of a segment of the spectrum (~400 nm) within one pulse ("spectrum-in-pulse" rather than the customary "point-by-point spectrum" technique[8]), a feature that is essential to the investigation of explosive ("one-time only") samples.

In the conductivity channel the current through the sample is recorded from the voltage drop across the oscilloscope input resistance, which is connected in series with the sample. When an S8-12 oscilloscope is used, the time resolution is 7 ns and is determined by the oscilloscope; for the S7-19 high-speed oscilloscope the time. resolution of the channel is limited by the parameters of the measurement cell and is —0.3 ns.

In the acoustic signal channel the sample is attached to the input window of an acoustic sensor in the form of a piezoelectric detector with an intrinsic time resolution ~1 ns. The signal from the acoustic sensor is sent to an oscilloscope.

The channels are synchronized by means of references pulses generated by the input of an initiating pulse to a detector (scattered light from a laser pulse incident on a pho-todetector, direct action of a laser pulse on the acoustic sensor, etc.). The time-referencing error limits of the signals of the various channels are ± 3 ns. A detailed description of the equipment configuration used in the investigation is given in Refs. 3,4.

3. RESULTS

3.1. Explosive conductivity

The explosion was initiated by a laser pulse. Uniform initiation was ensured by covering the interelectrode gap by a laser beam, the energy of exciting photons (λ = 1064 nm) being in the optical transparence range (the optical width of the band gap in silver azide ~3,5 eV, the thermal width ~1,5 eV[10]).

A typical profile of the explosive conductivity pulse is shown in Fig.2a. The simplest explanation for the observed kinetics is that the rise of conductivity in the first peak is associated with the still intact crystal (predetonation conductivity), the decay of the first peak corresponds to rupture of discontinuity of the sample due to growing stresses induced by decomposition and the next rise is related to the conductivity of explosion products (plasma).

In order to verify the above assumption the following series of experiments was carried out. The sample was mounted by its lateral face against the input window of the acoustic detector to allow one to synchronically measure both the acoustic signal and the conductivity signal. The onset of the sample deformation resulting in its mechanical fragmentation was determined from the leading edge of the acoustic detector signal. The sample conductivity preceding the leading edge of the acoustic signal (Fig.2b) corresponds to the intact sample, i. e. it can be identified as predetonation conductivity.

The concentration of conductivity electrons in the crystal $n \approx 5 \cdot 10^{20}$ cm^{-3} (Ref. 11) corresponds to the maximum values of the recorded conductivity 1000 $\Omega^{-1} \cdot cm^{-1}$ (Fig.2[c]) at $\mu = 10$ $cm^2 V^{-1} \cdot s^{-1}$ (Ref. 6). The resulting estimate of n as an approximation of characteristic values for metals indicates a very unusual state of the material in the predetonation phase, which can probably be regarded as a special kind of phase transi-

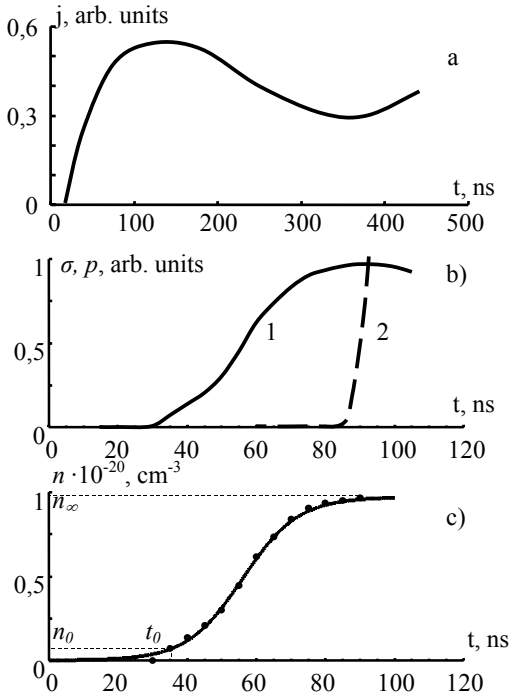

Fig. 2. Kinetics of AgN_3 whiskers explosive conductivity.
a – complete oscillogram of the current pulse,
b – initial site of explosive conductivity pulse (pre-explosive conductivity)
1 – conductivity
2 – leading edge of acoustic signal
c – kinetics approximation by equation (3). (solid line – the calculation according to the expression (3), points show the n values calculated on the basis of experimental σ values , t_0, n_0 are the time and concentration corresponding to the appearance of reliable registered current signal.

tion. It can serve as a reference point for an experimentally justified choice between the concepts of thermal and chain explosions of HMAs (Ref. 1).

As the thermal width of silver azide band gap is ~1,5 eV[11], the equilibrium concentration of electron-hole pairs is about 10^{-10} cm^{-3} at 523 K (the melting point of AgN_3 (Ref. 2)). Consequently, the experimental values of σ in the predetonation state unequivocally rule out the thermal mechanism of explosive decomposition and can be regarded as direct experimental proof that the explosion of HMAs is a chain reaction.

The simplest quantitative description of the kinetics of the type in Fig.2c is represented as:

$$\frac{dn}{dt} = \alpha \cdot n - \beta \cdot n^2 \qquad (1),$$

where n is the density of holes (electrons).

The solution of Eq. 2 at $n(t_0) = n_0$ is:

$$n(t) = \frac{\exp[\alpha \cdot (t - t_0)]}{n_\infty^{-1} \cdot \{\exp[\alpha \cdot (t - t_0)] - 1\} + n_0^{-1}} \quad (2)$$

where n_∞ is the density on the plateau, and t_0 and n_0 are the time and density at which the density attains a value that can be reliably measured. The value of n in Fig 2c is calculated from the relation: $\sigma = e \cdot n \cdot \mu$ with $\mu \approx 10$ $cm^2V^{-1}s^{-1}$.

It should be emphasized that parameters t_0, n_0 and n_∞ in Eq. (2) have been evaluated directly from the experimental curve and the only fitting parameter is α. For all the investigated samples the values α and β lie in the intervals 10^8 – 10^9 s^{-1} and 10^{-11} – 10^{-12} cm^3 s^{-1}, respectively.

The simplest interpretation for Eq. (1) whose solution is given by Eq. (2) is as follows. The growth (branching) of the chain is governed by a monomolecular process (αn), and its breaking by a bimolecular process (βn^2). It is reasonable to analyze the experimental values α and β in order to advance the a sensible hypothesis concerning the nature of corresponding processes. The simplest approach is to start with $\beta = \upsilon \cdot S_r$,, where υ is thermal electron (hole) velocity, and *Sr* – the cross-section of the process inducing the breaking of the chain. For $\upsilon \approx 10^7$ cm s^{-1} we have $S_r \approx 10^{-18}$ - 10^{-19} cm^2. These values are typical of indirect interband recombination[12], i.e., the simplest interpretation of bimolecular breaking of the chain, (βn^2), is the interband recombination of electrons and holes.

The simplest interpretation of the linear branching of a chain ($\alpha \cdot n$) is the trapping of a hole by a point defect. In this case $\alpha = \upsilon \cdot S_l \cdot N$, where υ is the thermal velocity, S_l

– the capture cross-section, and N – the density of defects. For $\upsilon \approx 10^7$ cm s^{-1} and $N \approx 10^{15}$ cm^{-3} (the typical density of cation vacancies in AgN3 whiskers) S_l was $\sim 10^{-14}$ cm^2, i.e. the characteristic capture cross-section for trapping by the attractive center.[13] Thus, the branching of the chain may be related to the trapping of a hole by the cation vacancy (the attractive center).

3.2. Explosive luminescence

The shape of the light pulse accompanying the explosive decomposition of HMAs (Fig.3) resembles that of the current pulse (Fig.2a) and suggests that this luminescence consists of two components: predetonation luminescence (the first maximum) and luminescence of the explosion products (the next rise). At any rate, the part of the luminescence preceding the onset of the acoustic signal (Fig. 3) is undoubtedly associated with the intact sample and can be identified as predetonation luminescence. This conclusion has been confirmed by the luminescence spectral composition at different stages of explosive decomposition.[14]

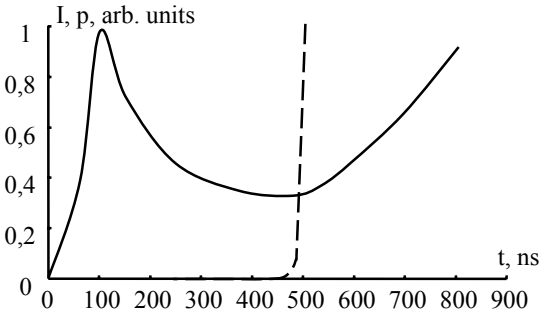

Fig. 3. Kinetics of AgN_3 whisker explosive luminescence (λ = 550 nm, the initiation was performed by laser pulse, crystal was mounted on a flat cell in contact with acoustic detector), solid line – light signal, dotted line - leading edge of acoustic signal..

Predetonation luminescence is of major interest. The spectrum of this luminescence (Fig. 4) or at least part of it cannot be described by the Planck formula, attesting to its nonthermal nature and identifying the light radiation as predetonation luminescence.[15]

Certain properties of this luminescence necessary for better understanding the nature and mechanism of explosive decomposition are as follows.

1. In all the objects the short-wavelength boundary of the luminescence lies in the optical transparency region. This result allows one to eliminate the photomultiplication process as a probable mechanism of hole multiplication discussed elsewhere[3].
2. A large part of the predetonation luminescence spectrum corresponds to photon energies grater than the HMA thermal band gap width (1 - 1,5eV). Thus, the luminescence discussed is hot luminescence.[15]

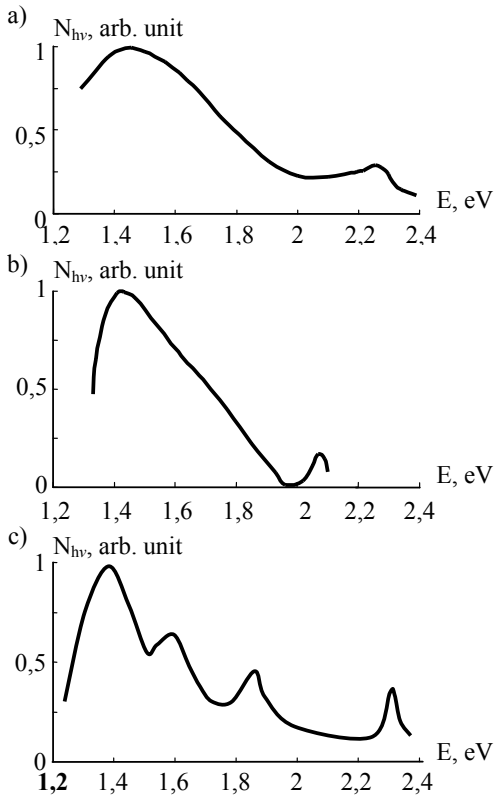

Fig. 4. HMA predetonation luminescence spectra of AgN_3 (a), $Pb(N_3)_2$ (b), TlN_3 (c)

3. Synchronous measurements of the predetonation conductivity and predetonation luminescence show that this luminescence is observed in the range of very high band charge carriers densities ($\sim 10^{20}$ cm^{-3})[16].

4. It has been shown that the mechanical fragmentation of a sample is preceded by partial melting. Consequently, predetonation luminescence is observed at close to melting point temperatures, at which luminescence is usually extinguished.[15]

The reabsorption-corrected luminescence kinetics is represented by a curve leveling off into a plateau (Fig. 5) and is very similar to the kinetics of the predetonation conductivity (Fig. 2). This similarity is more than outward appearance. The corrected luminescence kinetics as is the case for the predetonation conductivity kinetics is well approximated by the solution of the equation:

$$\frac{dI}{dt} = \alpha \cdot I - \beta \cdot I^2 \qquad (3)$$

which has the form

$$n(t) = \frac{\exp[\alpha \cdot (t - t_0)]}{I_\infty^{-1} \cdot \{\exp[\alpha \cdot (t - t_0)] - 1\} + I_0^{-1}} \qquad (4)$$

where t_0 is the time at which $I(t)$ attains a value I_0 that can be reliably measured, and I∞ is the value of $I(t)$ on the plateau. As in the case of the predetonation conductivity, the value of the constant α in Eqs. (3) and (4) lie in the interval $\alpha = 10^8 \div 10^9$ s^{-1} for different samples.

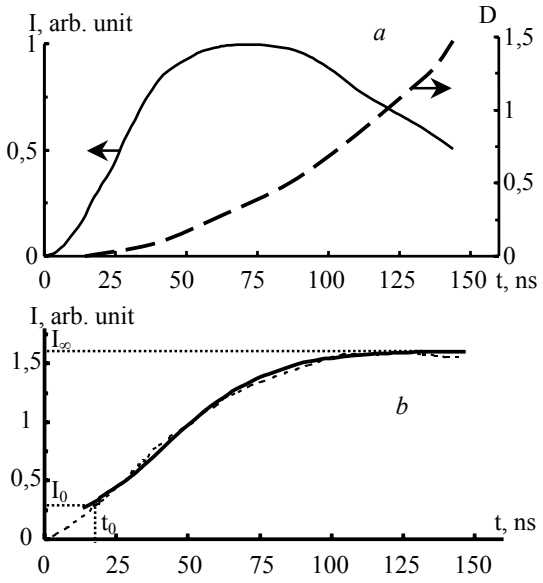

Fig. 5. Kinetics of AgN_3 whisker explosive luminescence (λ = 550 nm, the initiation was performed by laser pulse)
a – luminescence signal (solid line) and optical absorption (dotted line),
b – luminescence kinetics corrected for reabsorption. Dotted line shows the calculation of luminescence signal and optical density by experimental values, solid line – the calculation by equation (4), t_0 is the time at which luminescence signal is a reliable registered I_0 value.

The present authors suppose that the coincidence of both predetonation luminescence and predetonation conductivity kinetics is very important fact confirming that they reflect the kinetics of the basic process: explosive decomposition. This must be taken into account in constructing a model of predetonation luminescence and explosive decomposition on the whole.

The predetonation luminescence properties enable one to considerably limit the range of possible models of this phenomenon. Above all, the condition $\hbar\omega > E_g$ and the absence of the temperature extinction of this luminescence rule out all types of luminescence associated with local centers.[15] The comparison of the spectra of predetonation luminescence with the band structure data[15] also serves to rule out such types of fundamental luminescence as edge, exciton and cross-luminescence.[17]

Thus, the only luminescence we should discuss is the intraband luminescence due to radiative transitions of hot electrons and holes in the conduction and the valence bands, respectively. However, the present authors failed to discern any reasonable correlation between the band structure of the objects under investigation and the predetonation luminescence spectra, which is one of the basic approaches used to identify the intraband luminescence.

An altogether different picture emerges when the valence band is assumed to contain quasi-local hole states. If a level corresponding to a quasi-local hole state is pre-

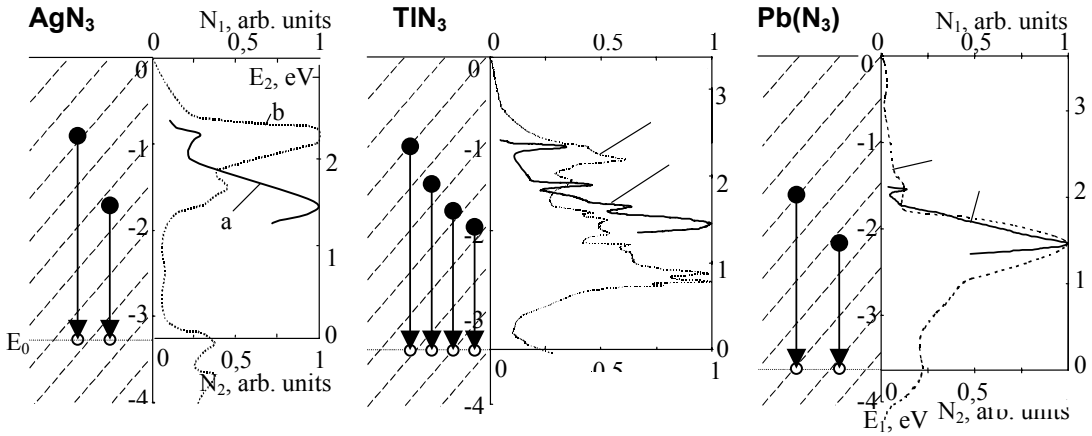

n of the predetonation luminescence (a) and the density-of-states in the valence band (b) for $(N_3)_2$.
E_1 or density-of-states
E_2 and N_2 - the scale for the predetonation luminescence spectrum, E_0 - the position of a quasi-local level corresponding to the best correlation between the predetonation luminescence spectrum maxima and the density-of-states peaks. Optical transitions of electrons from the valence band into a quasi-local state are shown by arrows.

sent in the interior of the valence band at a distance of 3,2 eV for AgN_3, at 3,4 eV for TlN_3, and at 3,6 eV for PbN_6 from the top of the valence band, a distinct correlation is observed between the luminescence maxima and the density-of-state peaks (Fig. 6). The present authors have failed to obtain an analogous correlation, for a level corresponding to a quasi-local state in the conduction band.

All this has enabled us to propose intraband radiative transitions of valence band electrons into quasi-local hole states (QLS) situated in the depth of the valence band as a model of predetonation luminescence (Fig. 6). Inasmuch as the lifetime of hole in quasi-local state is at most ~ 10^{-14} s[18] these states must be continuously generated during explosive decomposition.

The analysis of the results 3.2-3.3 allowed us to propose the model of the chain reaction for predetonation processes providing the explosive decomposition of heavy metal azides.[16,19] The main idea of the model for the chain link implies the formation of OLS in the valence band as a result of the reconstruction of a center arising from the trapping of a hole by a cationic vacancy. The delocalization of a hole from QLS results in the formation of hot band hole providing the multiplication of electrons and holes, which results from the impact ionization.

3.3. Early stages of explosive decomposition

A simple character of predetonation conductivity and luminescence kinetics is provided by deeping of competitive channels, i.e. by "burning-out" competitive trapping centers as a result of electron and hole localization on those centers at the concentration of band charge carriers $n > 10^{17}$ cm^{-3}. However, some deviations from the simple law (2) should be expected for early stages of the process ($n \leq 10^{17}$ cm^{-3}) due to the influence of competitive channels, i.e. the trapping of holes on lattice defects.

In this connection, we've investigated the early stages of predetonation conductivity. A signal measured was registered simultaneously with two oscillographs S7-19. A "lacing" of oscillograms obtained with different sensitivity (and different sweeps if needed) allows us to expand dynamic range of measuring channel to two orders of

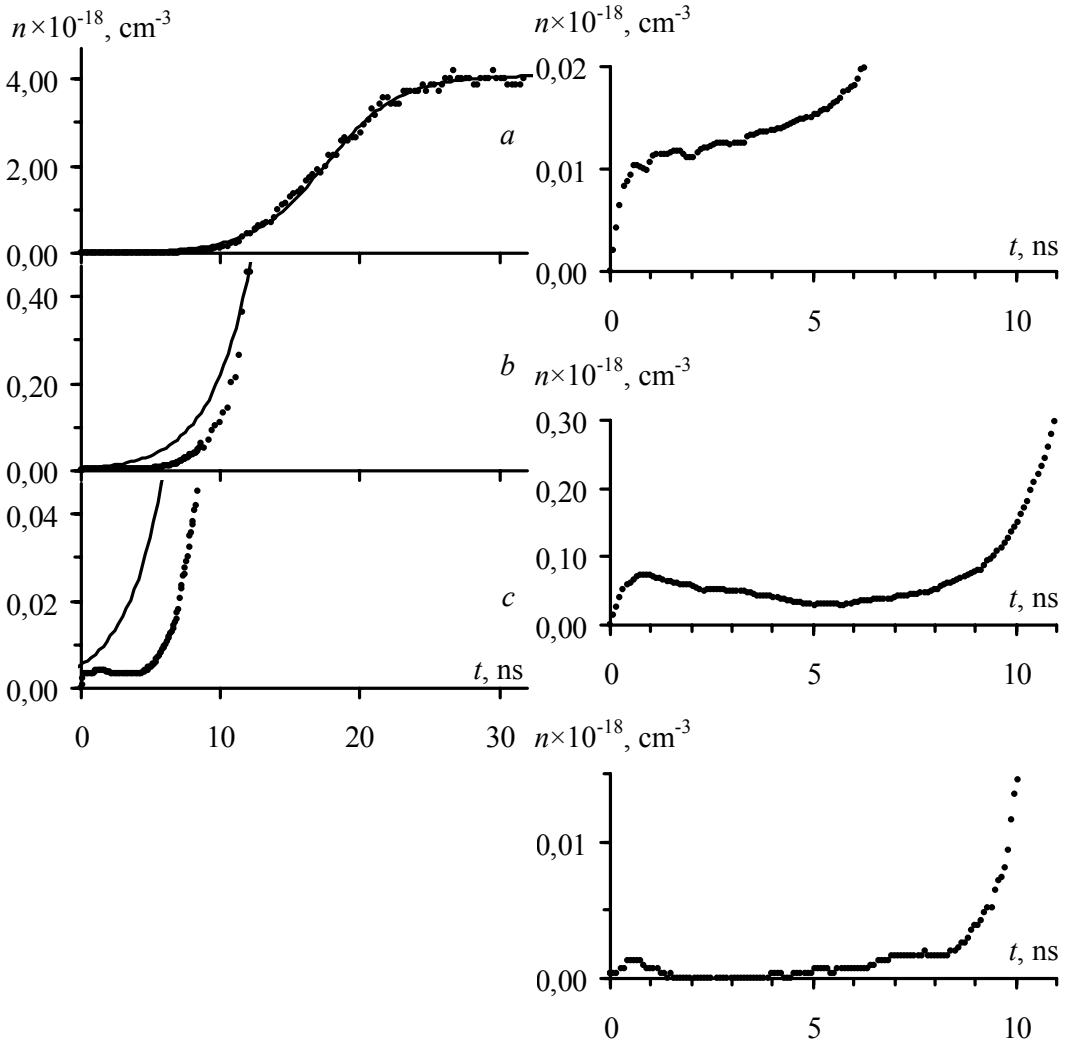

magnitude. Twenty samples of silver azide whiskers were investigated. The initiation was performed by a laser pulse.

Typical curves for concentration of band charge carriers vs. time are presented in Fig. 7 and Fig. 8. Fig. 7a shows that conductivity kinetics is well described by the expression (2) at n $>10^{17}$ cm^{-3}. For all samples investigated the values α and β lie in the intervals 10^{8} – 10^{9} s^{-1} and 10^{-11}– 10^{-12} cm^{3} c^{-1}, respectively. The above results agree well with Fig. 2c.

The initial parts of kinetic curves (Fig. 8) are of special interest. Fig. 8 shows a more complicated character of initial stages than a character of kinetics described by expression (2).

The following features should be discussed.

1. Difference between kinetic curves for different samples at early stages (Fig. 8) is greater than that for developed process described by expression (2).
2. The initial maximum, apparently, corresponding to a pulse of photoconductivity initiated by a laser pulse is observed in all the curves.
3. The curve corresponding to extrapolation of the law (2) to lower times lies higher than the experimental curve (Fig. 7). Further coincidence between extrapola-

tion curve and experimental kinetics (Fig. 7) is provided by the fact that the latter rises faster in the initial part.

As was shown previously,[20] the chain process should develop slower than according to the law (2) owing to consumption of holes by competitive channels. The latter fact can explain a great diversity of experimental data due to various concentrations of defects in different samples (the stage sensitive to structure[14]). However, we can't explain faster rise in conductivity, taking into account only this fact. We propose that the rise above probably related to the overlapping of reaction zones, forming continuous conductivity channel in a sample. Nidal nature of HMA initiation in the course of HMA slow decomposition has been proved experimentally (Ref. 6) and areas around dislocations have been shown to be reaction zones (Ref. 19).

Previously,[20] the initiation of lead azide by laser at free-running lasing and modulated lasing modes at near-threshold energy using high-speed photography has been investigated. It has been shown that initiation at free-running lasing mode always occurs in localized sites. For modulated lasing mode this fact has not been observed. Nevertheless, the authors (Ref. 20) have proposed on the basis of indirect data that the reaction in that case also can begin simultaneously in several local sites disposed at a short distance. Time resolution of the apparatus used by authors (Ref. 20) was ~ 250 ns only. Therefore, the investigation of topography dynamics for HMA explosive glow, using modern experimental techniques of nanosecond and subnanosecond time resolution was of special interest.

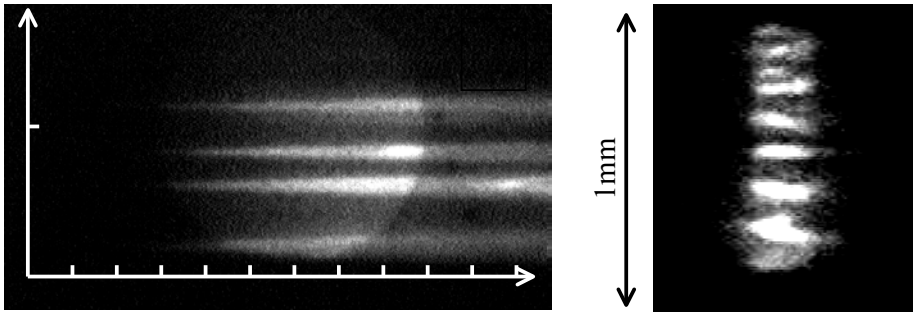

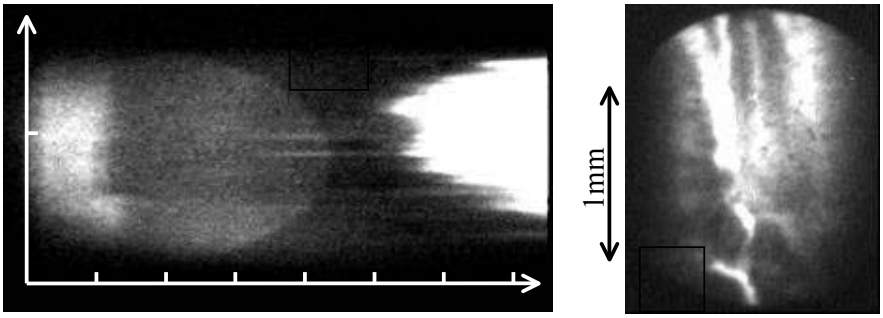

An enlarged image of silver azide whisker was transmitted by optical objective to photoelectric cathode of streak-camera "View 2A". Spatial resolution was 50 mm.

Initiation was performed by a laser pulse. The image of a sample glow under initiation near threshold of explosive decomposition is presented in Fig. 9. The glow is localized in separate luminous points (Fig. 9a). It should be emphasized that we concerned with predetonation luminescence at the density of energy ~ 5 mJ/cm^2. When the density of excitation energy is elevated to 100 mJ/cm^2 homogeneous glow in a sweep is observed (Fig. 10), the fast first component occurs in predetonation glow. Intensity of the latter depends on laser pulse energy.

The results obtained show that development of explosive decomposition has expressed heterogeneous character near initiation threshold under the effect of even ultrashort laser pulses. We believe that HMA explosive decomposition is of a chain nature and the results of the present paper give strong evidences for it. So we do not consider a relation of areas of primary initiation with strongly absorbed microcenters as stated elsewhere (Ref. 20).. We propose that these areas have increased local concentration of structure defects (e.g. areas near dislocations). The results presented elsewhere (Refs. 6, 19) give an evidence for the above assumption. The authors (Ref. 6) have stated that HMA slow decomposition in electric and magnetic fields occurs near dislocations. Furthermore, theoretical calculations predict appreciable constriction of band gap near dislocations for high explosives (Ref. 19).

It is clear, that the above considerations on the nature of local areas of HMA initiation are preliminary ones and require further experimental testing.

4. CONCLUSION

By way of conclusion the present authors would like to call attention to a certain fundamental aspect of the problem, which far transcends the problem of elucidating the mechanism of HMA explosive decomposition. The information presented convincingly demonstrates a very interesting possibility for chemical reactions to be realized in solids. A necessary condition for the chemical reaction in liquids and gases is a real migration of reactants towards each other. In solids it is quite different. Electron excitations migrate and their trapping at certain sites of the crystal lattice (at structural or impurity defects) gives rise to actual radicals at the necessary site. Thus, a sufficiently lengthy migration of real heavy particles (usually by diffusion) is replaced by a faster migration of electron excitations. Far-going prospects to utilize this promising possibility have not been fully appreciated in modern solid-state physics and chemistry.

REFERENCES

1 Bowden F.P., Yoffe A.D. Fast reaction in Solids, Butterworths, Scientific Publications, London (1958), p. 242.

2 Energetic Materials, Edited by H.D. Fair, R.F. Walker, New York, Plenum Press, V. 1, (1987), p. 501.

3 Aduev B.P., Aluker E.D., Belokurov G.M.,Krechetov A.G. Russian Physics Journal, **39**(11), 1135 (1996).

4 B.P. Aduev, E.D. Aluker, V.G. Kriger, Yu.A. Zakharov. Solid State Ionics, **101-103**, 33 (1997).

5 Kriger V., Kalensky A. Chem. Phys. Reports, **14**(4), 556 (1995).

6 Krascheninin V.I., Kuzmina L.V., Zakharov Yu.A., Stalinin A.Yu. Chem. Phys. Reports, **14**(4), 126 (1995).

7 Alexandrov E.I., Voznyuk A.G. Fizika Goreniya i Vzryva. 19(4), 143 (1983), (in Russian).

8 E.D. Aluker, V.V. Gavrilov, R.G. Deich, S.A. Chernov, Bystroprotekayushcie radiatsionno-stimulirovannye protsessy v shcelochnogaloidnykh kristallakh, - Riga. Zinantne. 1987, p. 183, (in Russian).
9 Kurakin S.I., Diamant G.M., Pugachev V.M. Izv. AN SSSR. Neorganicheskie materialy, **26**(11), 2301 (1990), (in Russian).
10 Gordienko A.B., Zhuravlev Yu.N., Poplavnoi A.S. Phys. Stat. Sol.(B), **198,** 707, (1996).
11 Aduev B.P., Aluker E.D., Belokurov G.M., Krechetov A.G. JETP Lett. **62 (3)**, 203, (1995).
12 Ya. E. Pokrovskiy (Ed.) Radiative recombinations in semiconductors. - Moscow, Nauka. 1972, p.304, (in Russian).
13 A.M. Stoneham. Theory of Defects in Solids, Clarendon Press, Oxford, 1975, p. 731.
14 B.P. Aduev, E.D. Aluker, A.G. Krechetov and A.Yu. Mitrofanov. Phys. Stat. Sol. B, **207**, 535 (1998).
15 V.P. Gribkovskii Teoriya pogloshcenia i ispuskaniya sveta v poluprovodnikakh. - Minsk. Nauka i tekhnika. 1975. p. 463, (in Russian).
16 B.P. Aduev, E.D. Aluker, G.M. Belokurov, Yu.A. Zakharov, A.G. Krechetov, *JETP* **116**,5 (11), 1676, (1999)
17 Rodnyi P.A. Fisika tverdogo tela **34**(7), 1975 (1992), (in Russian).
18 F. Bassani, G.P. and Parravicini. Electronic States and Optical Transitions in Solids. - Pergamon Press. New York. 1975, p. 391.
19 Kuklja M.M., Aduev B.P., Aluker E.D., Krasheninin V.I., Krechetov A.G. and Mitrofanov A.Yu. Journal of Applied Physics. **89**(7), 4156, (2000).
20 Hagan J.T., Chaudhri M.M. J. Mat. Sc. **16**(8), 2457, (1981).